ECS Journal of Solid State Science and Technology, **3** (10) R189-R194 (2014)
2162-8769/2014/3(10)/R189/6/$31.00 © The Electrochemical Society

Luminescent and Structural Characteristics of Y_2O_3:Tb^{3+} Thin Films as a Function of Substrate Temperature

G. Alarcón-Flores,[a,z] M. García-Hipólito,[b] M. Aguilar-Frutis,[a] S. Carmona-Téllez,[c,*] R. Martinez-Martinez,[d] M. P. Campos-Arias,[a] M. Jiménez-Estrada,[e] and C. Falcony[f]

[a]*CICATA-IPN, Colonia Irrigación 11500, Mexico*
[b]*IIM-UNAM, Coyoacán 04150, Mexico*
[c]*Instituto de Física, UNAM, Coyoacán 04150, Mexico*
[d]*Universidad Tecnológica de la Mixteca, Huajuapan de León Oaxaca 69000, Mexico*
[e]*Instituto de Química, UNAM, Coyoacán 04150, Mexico*
[f]*Departamento de Física, CINVESTAV, Gustavo A. Madero 07000, Mexico*

An inexpesive synthesis of terbium and yttrium β diketonates from acetylacetone and metal chlorides was carried out. Later, the β diketonates were used as precursors for the synthesis of Y_2O_3:Tb^{3+}thin films by the ultrasonic spray pyrolysis technique. The β diketonates are sometimes preferred as precursors for thin films because they lead to high quality films; such as a very low surface roughness and a high homogeneity. With the later idea films of Y_2O_3:Tb^{3+} were deposited on c-Si substrates at temperatures in the 400–550°C range. Yttrium β diketonate was used as precursor of Y_2O_3 host lattice and terbium β diketonate was used as source of Tb^{3+} activator. The optical and structural characterization of the thin films were carried out by means of photoluminescence (PL) and cathodoluminescence (CL) spectroscopies, infrared spectroscopy (IR), ellipsometry, atomic force microscopy (AFM), energy dispersive spectroscopy (EDS), and X ray diffraction (XRD). From PL and CL spectra, the luminescence intensity depended strongly on substrate temperature, the thickness of the film, and the Tb^{3+}-activator concentration. Y_2O_3:Tb^{3+}thin films exhibited one main band centered at 547 nm which was due to the well-known $^5D_4 \rightarrow {}^7F_5$ electronic transition. In addition, a concentration quenching of the luminescence intensity was observed. At high temperatures the cubic crystalline phase of Y_2O_3 was obtained as well as a reduction of organic residues. Additionally, at elevated temperatures,a low average surface roughnesswas obtained in the films with a high density and a high transparency.

Manuscript submitted May 30, 2014; revised manuscript received July 7, 2014. Published August 8, 2014.

Metalorganic complexes such as metal β diketonates, also called acetylacetonates, are of great interest because of their excellent chemical and physical properties. Principally,because their high volatility and low decomposition temperature, they are very important for several scientific and technological areas. It has been suggested that a chemical vapor deposition is followed when using β diketonates in the deposition of several types of thin oxide films, such as dielectric layers, semiconductors and superconductors, some of them carried out in industrial processes in large scale.[1–3] Most methods that involve deposition processes from metallorganic vapor lead to thin films with low surface roughness, better adhesion to the substrate, dense and relatively clean, as compared with films synthesized by the use of inorganic sources such as metal chlorides or nitrates.[4,5] A relatively inexpensive method for the synthesis of metal oxides thin films is the ultrasonic spray pyrolysis (USP) method. This method has several advantages compared with others deposition techniques, such as: chemical vapor deposition, sputtering deposition, pulsed laser deposition.[6] Wide band-gap metal oxides such as: Al_2O_3 (gap = 5.8 eV),[7] HfO_2 (gap = 5.4 eV),[8] Y_2O_3 (gap = 5.5 eV)[9] are often used as host lattice to incorporate optical activator ions, because of their high chemical stability, high resistance to cathode rays and high thermal stability (melting points higher than 2300°C). Yttria (Y_2O_3) is a cubic crystalline material with high melting temperature (2410°C), large transmittance (from 280 nm to 8 μm),[10] and high crystalline stability.[11] Y_2O_3 host lattice is important for the manufacture of scintillators, lasers, optical fiber and as nanocrystalline phosphors; due to quantum size confinement, the luminescent properties of nanocrystalline phosphors might be quite different from their bulk counterpart, so their properties can be improved to expand their applications. Due to a maximum field gradient before charge drain, a maximum voltage (about 1 kV) may be applied in devices for flat panel displays applications (FED, and PD), which is much lower than the one applied in the normal display devices (5 kV).[7] A nanocrystalline phosphor generally has a high efficiency which can be achieved with low voltages. Therefore, they are ideal candidates for flat display devices.[8] In addition, high definition televisions (HDTV) require phosphors with small particle size, distribution size uniformity and high light intensity without saturation.[7]

In the present work we report an inexpensive and fast synthesis of terbium and yttrium β diketonates from acetylacetone and terbium and yttrium metal chlorides to subsequently prepare thin films of Y_2O_3:Tb^{3+} by means of ultrasonic spray pyrolysis technique. The films resulted with a considerable low surface roughness, dense, and well adhered to the substrates. The PL and CL spectra shown a strong dependence of the luminescence intensity with the substrate temperature. The high temperature yielded a considerable reduction of the diketonates precursors and led to the formation of polycrystalline Y_2O_3. Also, luminescence intensity was influenced by Tb^{3+}-activator concentration and a concentration quenching was observed.

Experimental

Synthesis of yttrium β diketonate.— For the synthesis of yttrium β diketonate a solution containing $Y(NO)_3$ was prepared. For this purpose a solution was prepared with 3.83 g of $Y(NO)_3$ that were dissolved in a solvent containing 15 mL of distilled water and 10 mL of methanol. We then placed the solution in an ice bath and added 3 mL of acetylacetone and 3 mL of propylene oxide in a dropwise manner. We later added concentrated ammonium hydroxide to the solution up to it reached a pH of 7 (1.5 mL of ammonium hydroxide were added to the solution). The solution was then stirred for 45 minutes and after that time a light yellow powder precipitated, which was then vacuum filtered. This powder was then dried at 80°C for four hours. This method has been reported by W. Sheng-Yue, and T. E. Banach.[11,12] The obtained powder was identified as yttrium β diketonate by means of proton nuclear magnetic resonance ^{1}H-NMR (Bruker-Avance System 300 MHz instrument), Mass Spectrometry MS (JEOL AX505HA spectrophotometer), and infrared spectroscopy IR (Perkin Elmer spectrum one). Its spectroscopic data are shown below, and the structural formula is shown in Fig. 1.[11,12]

^{1}H-NMR (p.p.m): 1.74 (6H, s), 5.21 (1H, s).

MS (m/z): M^+ 386(44.6%), 371 (3.1%) (M^+ -15), 287 (100%) (M^+-99).

IRνmax(cm^{-1}) 1570 ν (C=O)and ν(C=C), 525 ν (C=C) and ν(C=O), 535 (MO)

*Electrochemical Society Student Member.
[z]E-mail: alar_fbeto@yahoo.com

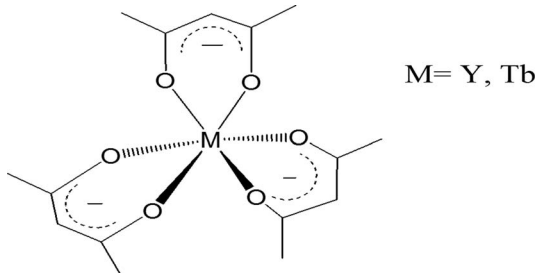

Figure 1. Structural formula of yttrium and terbium β diketonate.

Synthesis of terbium β diketonate.— In the case of terbium β diketonate, its synthesis was similar to the one used for yttrium β diketonate, as described in references 11 and 12. For this purpose, terbium chloride was used as raw material. The spectroscopic data of IR and 1H-NMR of terbium β diketonate were similar to the ones found in yttrium β diketonate. However the Mass Spectroscopy data were different because the terbium β diketonate molecular ion (M^+) was different (equal to 456). The molecular fragmentations were similar to the ones found in yttrium β diketonate.[4]

Synthesis of Y_2O_3:Tb^{3+} thin films.— The Y_2O_3:Tb^{3+}thin films were synthesized by ultrasonic spray pyrolysis. In the spray pyrolysis technique an atomized precursor solution is directed downward at the heated substrate, which upon decomposition and oxidation reaction forms a metal oxide thin film on top of the substrate. In this case the precursor solution was prepared with yttrium β-diketonate and the terbium β-diketonate. The spray pyrolysis technique is considered a low cost deposition technique for obtaining high quality thin films of several metal oxides. In our work, N, N-dimethylformamide (DMF) [C_3H_7ON, JT Baker and purity of 99.96%] was used as solvent, and a 0.03M solution of yttrium β diketonate was prepared by dissolving 2.32 g of it in 100 mL of DMF. Terbium β diketonate was added to the precursor solution in different atomic percentages [0.0, 2.0, 5.0, 10.0 and 15.0 at%], relative to the yttrium content in the initial solution. The films were deposited on crystalline silicon substrates, of size 1.5 $\times$ 1.5 cm^2, and on quartz substrates of the same size.

The substrate temperature during deposition was fixed at 400°C, 450°C, 500°C, and 550°C. A molten tin bath was used to achieve the required temperature, on top of which were placed the silicon or quartz substrates. The temperature of the molten tin bath was electronically controlled. The deposition time was of 15 minutes in all cases and air was used as carrier gas during for the spray deposition. Commercial ultrasonic humidifiers were used to get the atomized precursor solution. Cathodoluminescence measurements were performed in a stainless steel vacuum chamber with a cold cathode electron gun (Luminoscope, model ELM-2 MCA, RELION Co.). The thin films were placed inside the vacuum chamber and evacuated down to $\leq 10^{-2}$ Torr. The electron beam was deflected through a 90 ° angle to focus onto the luminescent film normal to the surface; the diameter of the electron beam on the film was of 3 mm approximately. The emitted light was collected by an optical fiber and fed into a SPEX Fluoro-Max-Spectrofluorometer. The applied current of the electron beam was 0.05 mA with an accelerating voltage in the range from 3 kV to 10 kV. The photoluminescence spectra were obtained with the spectrofluorometer mentioned above. All the luminescence measurements were performed at room temperature. A Siemens D-5000 X-ray diffraction system with CuK_α ($\lambda = 1.5406$ Å) was used for the determination of the crystalline structure. Nanocrystalline sizes of films were estimated following the Scherrer's formula: $T = \frac{0.9\lambda}{B\cos\theta_B}$.

Where T represents crystallite size, λ represents the wavelength of CuK_α radiation and *B* represents corrected half width of the diffraction peak. Therefore these sizes were evaluated based on the full-width at half-maximum (FWHM). Optical transmission spectra were obtained from the films deposited on the quartz substrates. An UV-vis spectrophotometer (Cary 50) in the 200–900 nm range was used for this purpose. The surface morphology of the films was observed by Atomic Force Microscope (Veeco CP research). Finally, an LSE Stokes Gaertnerellipsometer was used to estimate the index of refraction of the films.

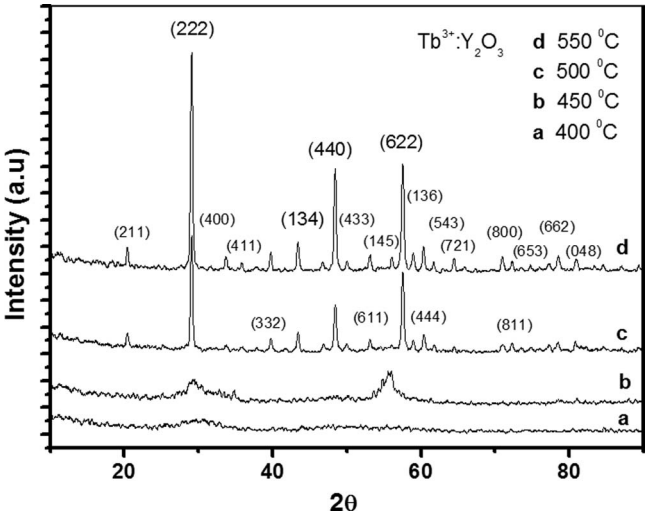

Figure 2. Diffractograms of Y_2O_3:Tb^{3+} thin films at different temperatures.

Results and Discussion

Fig. 2 shows the X-ray diffractograms for samples deposited at different temperatures, these diffractograms show that the films are amorphous when deposited at 400°C and remain mostly amorphous at 450°C, but at 500° and 550°C they become polycrystalline presenting a Y_2O_3 cubic phase. The most intense peaks are centered at 29.04,43.29, 48.39, and 57.54 which correspond to the planes(222), (134), (440) and (622) respectively (JCPDS card number 43–1036) withlattice parameter of 10.604 Å. These peaks were used to estimate the crystalline grain size values of 23 and 24 nm for films deposited at 500°C and 550°C, respectively, using Scherrer's formula. IR spectra for these films are shown in Fig. 3, these present two overlapped bands which are located approximately at 1405 and 1525 cm^{-1}; assigned to δ (C–H) and ν_{as} (C=O) coupled with ν (C=C) vibrations,

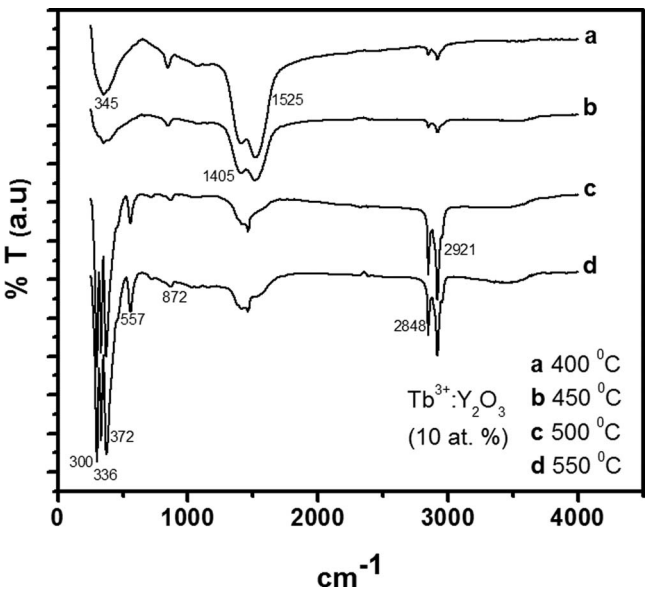

Figure 3. Infrared Spectra of Y_2O_3:Tb^{3+} (10 at%) thin films deposited at temperature range from 400 to 550°C.

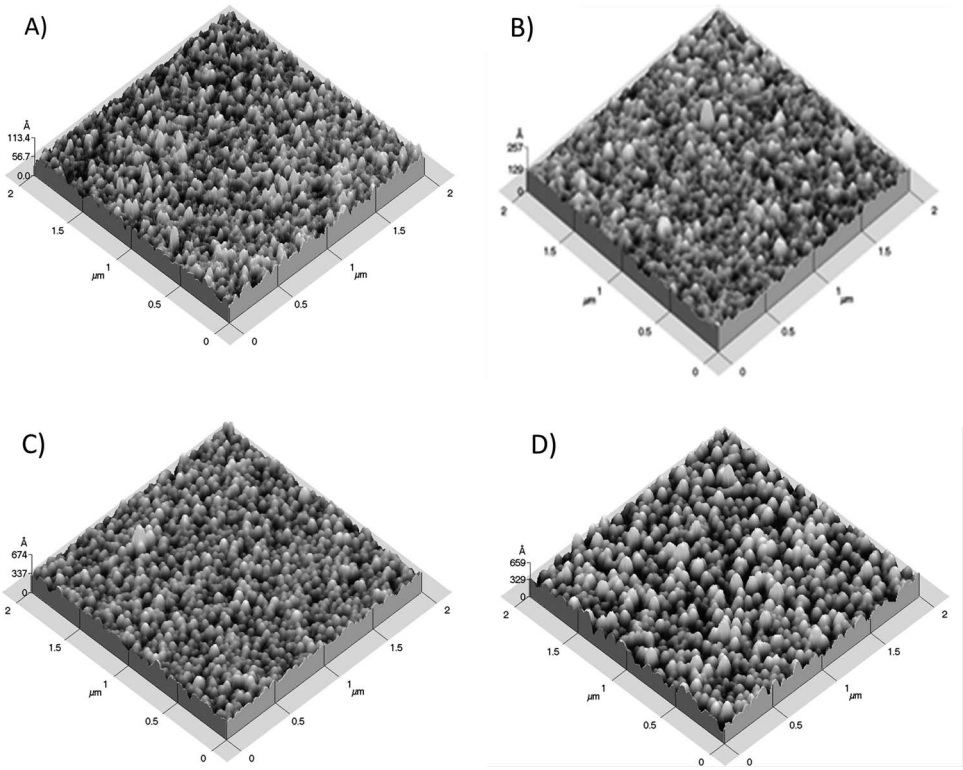

Figure 4. Atomic force microscopy (AFM) images for Y_2O_3:Tb^{3+} thin films deposited on silicon substrates at different deposition temperatures, a) Ts = 400°C, b) Ts = 450°C, c) Ts = 500°C and d) Ts = 550°C.

respectively[13,14] and a band at 872 cm^{-1} assigned to π (CH). The three bands are characteristic of the terbium and yttrium β diketonates and their presence in the films indicate incomplete decomposition of the precursors in particular at low temperatures. These bands decrease significantly with increasing temperature (at 500° and 550°C) although they are not completely removed at the highest temperature studied. The presence of organic residues in films deposited by using spray pyrolysis and sol-gel using organic precursors has been already reported in other works.[15–17] The IR spectra also present a broad band around 345 cm^{-1}, this band is increased and split, when the temperature is increased, in three well defined peaks at about 300, 336, 372 cm^{-1}, an another peak is also observed at about 557 cm^{-1}, all these peaks are assigned to Y-O stretching vibration so as expected from a Y_2O_3 host lattice.[14,18] This confirms the XRD results, showing that at temperatures for 500 and 550°C a well defined structure for Y_2O_3. The spectra show also, two bands located approximately at 2848 and 2921 cm^{-1}, these bands are assigned to stretching vibration mode of methyl group CH_3 (ν).[14] Finally, a weak band centered 3500 cm^{-1} corresponding to the O-H bonding is observed that most likely is due to H_2O molecules adsorbed on film surface.[4,17,18] Figure 4 shows the atomic force microscopy surface images of these films (with 10 at% of Tb^{3+}). The surface area shown corresponds to $4\mu^2$. All films in general show granular morphology with surface average roughness of 9.49 Å, 15.5 Å,47.5 Å and 76.2Å or 400,450,500, and 550°C respectively.

These values are very low if the thickness of samples is considered, which is between 1 and 1.5 μm. The films presents refractive indexes of ∼1.82 and ρ = 3.9247 g/cm^3. Densification was determined based on the refractive index change with the assumption of a linear relationship between density and refractive index; the relationship is given by $\rho = -4.784 + 4.785n$, where ρ is the density in g/cm^3 and n is the refractive index.[19]

Average roughness behavior is illustrated in Fig. 5 where the average roughness is ploted vs deposition temperature. The increase in roughness observed at 500°C could be due to the formation of the crystalline phase observed in the XRD diffractograms at these temperatures (Fig. 2).

The photoluminescence (PL) excitation spectrum obtained for aY_2O_3:Tb^{3+}film deposited at 500°C and with a concentration of 10 at% of Terbium chloride is shown in Fig. 6. This spectrum shows broad band in the wavelength range of 245 nm to 340 nm, and centered at 308 nm.This band could be attributed to a charge transfer (CT) process, from the 2p orbital of O to the 4f orbitals of Tb^{3+}.[20–22] It is noteworthy that the Stokes shift for all samples is 1.76 eV; 308 nm = 4.02 eV (excitation value) −547 nm = 2.26 eV (peak of greatest intensity of the emission spectrum); since these values are constant for

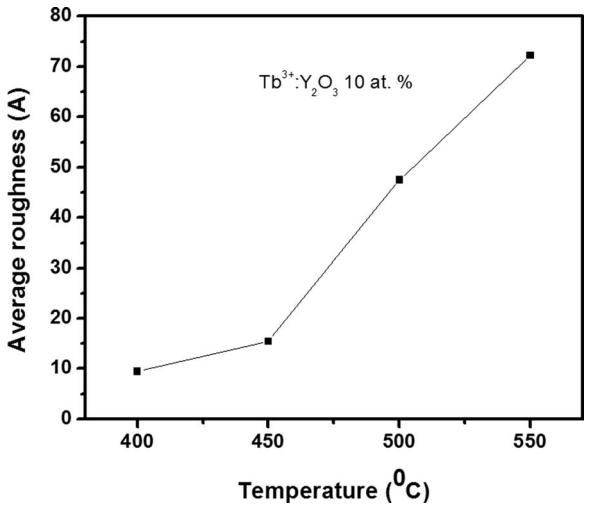

Figure 5. RMS Roughness variation of Y_2O_3:Tb^{3+} (10 at%) phosphors thin films with substrate temperature.

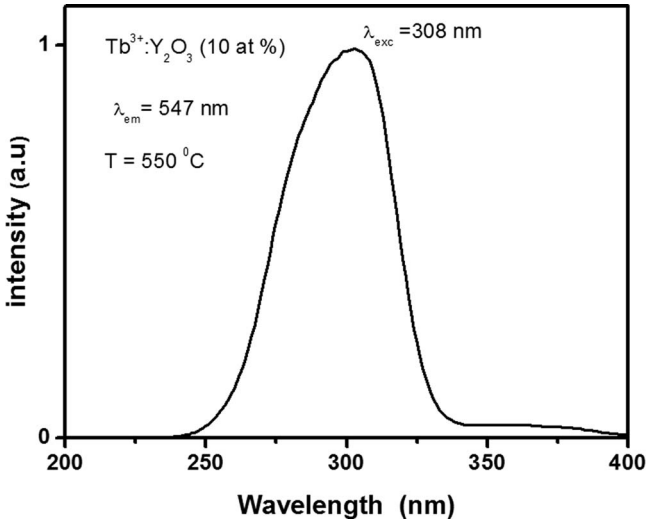

Figure 6. Excitation spectrum obtained for Y_2O_3:Tb^{3+} (10 at%) thin films synthesized at 550 °C. The emission wavelength was 547 nm.

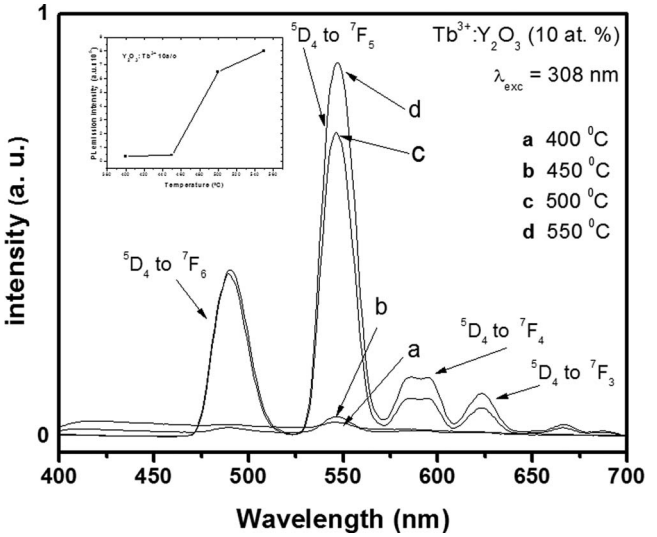

Figure 8. PL emission intensity spectra as a function of wavelength at different temperatures for (10 at%) Y_2O_3:Tb^{3+} thin films excited with wavelength of 308 nm.

all the deposition temperatures, and maintaining a constant concentration; it is just possible to observe changes in the intensities of the two spectra (excitation-emission) but not in the spectral structure.[23,24] Figure 7 shows the PL emission behavior for Y_2O_3:Tb^{3+}films (deposited at 550°C) as a function of the doping concentration. Four bands are present associated to the $^5D_4 \rightarrow {}^7F_j$(J = 6, 5, 4, 3) electronic transitions. The most intense radiation emission band is located at 547 nm ($^5D_4 \rightarrow {}^7F_5$) correspondingto the characteristic green color of the Tb related emission. The highest emission intensity was obtained for 10 at% of Tb^{+3} in precursor solution (10% Tb β diketonate in solution corresponds to about 1.78% of Tb by EDS measurements);while larger concentrations resulted in a concentration quenching of the luminescence emission,[5] these behavior is shown in the insetof Fig. 7, where the intensity of the main peak is plotted as a function of dopant concentration. Figure 8 shows the PL emission intensity for (10 at%) Y_2O_3:Tb^{3+}films deposited at temperatures of 400° to 550°C, using an excitation wavelength of 308 nm. Samples deposited at 400° and 450°C, present a quite weak photoluminescence. However, the photoluminescent emission is increased in films deposited at 500°C, and the maximum emission intensity corresponds to the film synthesized at 550°C, (as shown in the inset of Fig. 8). It is possible that a high deposition temperature helps to achieve a better stoichiometry and a high crystallinity of the host lattice, which could lead to a better incorporation of Tb^{3+} ions and as a consequence to an increase of the luminescence intensity. The latter result is in agreement to the X-ray diffraction analysis (see Fig. 2), that show an improved crystallinity of films deposited at these temperatures. The refractive index values of the films was close to 1.82, indicating dense films. Furthermore, EDS measurements reported a 2:3 ratio for yttrium and oxygen, respectively, indicating high quality films.

In order to determine if the Y_2O_3:Tb^{3+}films might have potential cathodic applications, cathodoluminescent measurements (CL) were performed in these films. Films deposited with 10 at% of Tb^{3+} and substrate temperature of 550°C were first analyzed using electron acceleration voltage in the 2 kV-10 kV range (Fig. 9). In these spectra it is observed that the highest intensity corresponded to the emission spectrum with the maximum acceleration voltage, 10 kV and in general the overall intensity was proportional to the acceleration voltage used. This results is expected since for higher acceleration

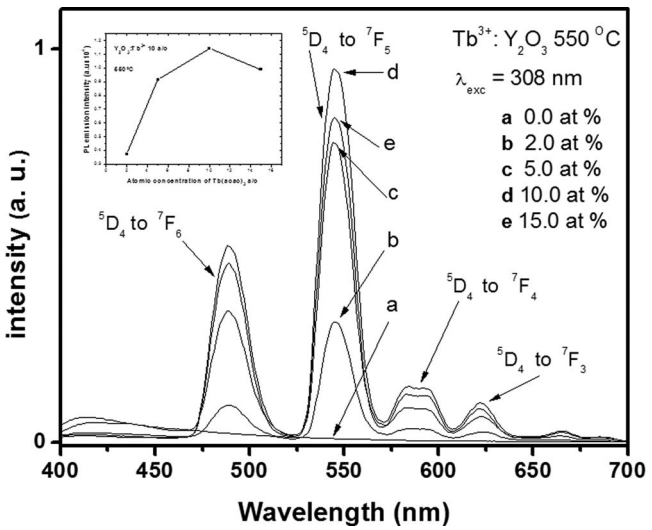

Figure 7. PL emission intensity spectra for Y_2O_3:Tb^{3+}thin films changing the doping concentration at 550°C, under excitation at 308 nm.

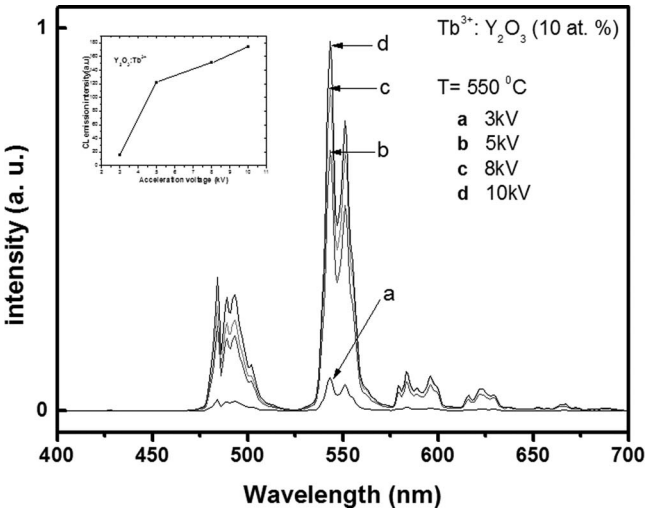

Figure 9. CL emission intensity spectra for (10 at%) Y_2O_3:Tb^{3+} thin films, varying electron acceleration voltage. The films were deposited at substrate temperature of 550°C.

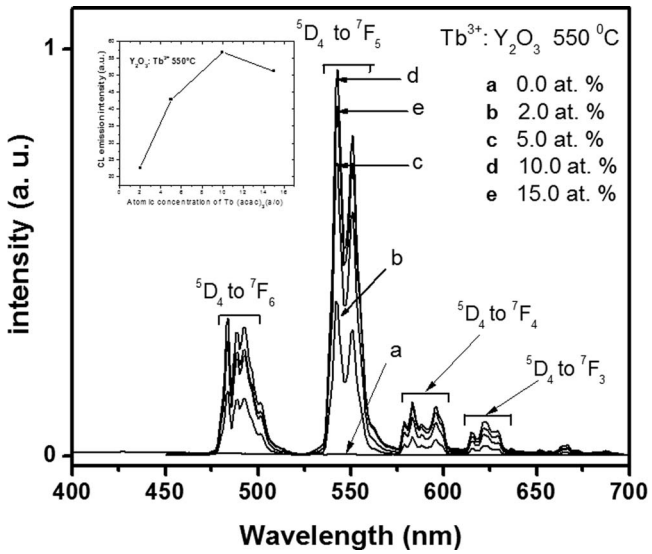

Figure 10. CL emission intensity spectra for Y_2O_3:Tb^{3+} thin films as a function of the wavelength varying doping concentration. The substrate temperature was of 550 °C and electron acceleration voltage was of 10 kV.

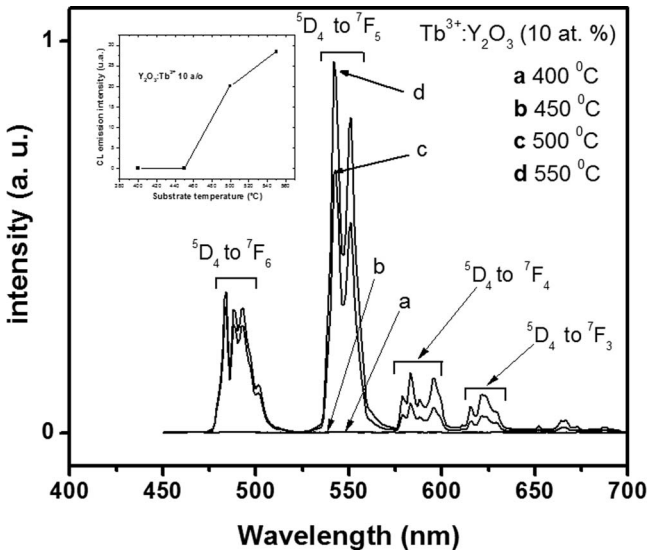

Figure 11. CL emission intensity spectra for Y_2O_3:Tb^{3+} thin films as a function of the wavelength varying the substrate temperature and electron acceleration voltage was of 10 kV.

voltage, the electrons penetrate deeper in the material producing more electron-hole pairs which in turn excite more luminescent centers due to their interaction with a larger volume of the luminescent material. Figure 10 shows CL emission intensity spectra for Y_2O_3:Tb^{3+}films as a function of the wavelength for doping concentration in the range from 0.0 at% to 15 at%. The films were deposited at 550°C and the applied electron accelerating voltage was 10 kV. The emission bands of cathodoluminescence are similar to the emission bands of photoluminescence also it was observed since the four bands $^5D_4 \rightarrow {}^7F_j$(J = 6, 5, 4, 3) have high J values[20] the crystal field splits the levels in several sublevels, due to the higher luminescence intensity produced by the electron beam, the CL spectra were measured with better resolution, which allowed for the observation of the the crystal field splits; it is known that the spectroscopic levels of trivalent rare earth ions in a crystal split under the influence of an asymmetric electric field produced by impurities or other defects in the crystal.[25] In addition, when the doping concentration is incremented at 15 at% of Tb^{3+} in the spraying solution, concentration quenching is observed, (inset of Fig. 10, CL emission intensity). Moreover, the emission inhibition can also be caused by local heating by bombardment of electrons, Auger effect, among others.[26] CL emission intensity spectra for Y_2O_3:Tb^{3+}films as a function of the wavelength varying the substrate temperature are shownin Figure 11. As the substrate temperature is increased, the CLemission intensity was also incremented. As mentioned for the photoluminescence results, this result suggest that at temperatures of 400° and 450°C the very weak emission might be due to the amorphous nature of these films as the X-ray results indicate (Fig. 2). The polycrystaline characteristic of the films obtained at temperatures of 500° and 550°C, on the other hand, seems to have a great influence on the luminescence characteristics of these films as revealed by the results of both photoluminescence and cathodoluminescence. Another possible cause of the weak or absent luminescence in films deposited at 400° and 450°C can be concluded from the infrared spectroscopy results presented in Figure 3, in which the incomplete reaction of the precusors is evidenced by the presence of the peaks associated with the organic residues in these films. These residual organic functional groups present into the films could be responsible for their degraded photo and cathodoluminescence emissions,[4] the reduction of these bands with increasing temperature indicate that the organic residues are reduced and consequently the PL and CL emissions intensity increase as observed in the Figs. 8 and 11.

Conclusions

Y_2O_3: Tb^{3+} films were synthesized at different substrate temperatures and with different concentrations of dopant using the ultrasonic spray pyrolysis technique. The temperature of deposition and the structural characteristics of the films influenced strongly the PL andCL emission intensities. Films synthesized at low temperatures presented large amount of organic residues and an amorphous structure that impared their luminescence emission, while those synthesized at high temperatures presented lower amount of organic residues and a polycrystalline structre that favored a strong luminescent intensity. The luminescence spectra presented a dominant peak located at 547 nm corresponding to the $^5D_4 \rightarrow {}^7F_5$ electronic transitions associated with Tb^{3+} ions. Also they revealed that the best experimental conditions to obtain the maximum emission intensity was a 10% of terbium in the precursor solution and deposition temperature of 550°C. A concentration luminescence quenching effect was observed at doping percentage greater than 10%. The films obtained at high deposition temperatures presented a maximum average surface roughness of 62 Å. The films presented in this work were dense, and show an index of refraction 1.82, as well as a high transparency in the visible range of the electromagnetic spectrum, suggesting the possibility to be applied in electroluminescent devices.

Acknowledgments

The authors thank warmly to SIP-IPN and DGAPA-UNAM for the financial support through the scientific research projects (Grant Nos. 20130236, 20130153, 20140458, and 20140459).

References

1. Albert G. Nasibulin, Esko I. Kauppinen, David P. Brown, and Jorma K. Jokiniemi, *J. Phys. Chem. B* **105**, 11067 (2001).
2. M. Aguilar-Frutis, G. Reyna-García, M. García-Hipólito, J. Guzmán-Mendoza, and C. Falcony, *J. Vac. Sci. Technol.* **A22**(4), 1319 (2004).
3. G. Alarcón-Flores, M. Aguilar-Frutis, C. Falcony, M. García-Hipólito, J. J. Araiza-Ibarra, and H. J. Herrera-Suárez, *J. Vac. Sci. Technol. B* **24**(4), 1873 (2006).
4. G. Alarcón-Flores, M. Aguilar-Frutis, M. García-Hipólito, J. Guzmán-Mendoza, M. A. Canseco, and C. Falcony, *J Mater Sci* **43**, 3582 (2008).
5. R. Martinez-Martinez, E. Yescas, E. Alvarez, C. Falcony, and U. Caldiño, *Advances in Science and Technology* **82**, 19 (2012).
6. Jun Yeol Cho, Ki Young Ko, and Young Rag Do, *Thin Solid Films* **515**, 3373 (2007).
7. C. Falcony, A. Ortiz, J. M. Dominguez, M. H. Farias, L. Cota-Araiza, and G. Soto, *J. Electrochem. Soc.* **139**(1), 267 (1992).
8. J. Aarik, H. Mändar, M. Kira, and L. Pung, *Thin solid films* **466**, 41 (2004).

9. V. Swamy, N.A. Dubrovinskaya, and L.S. Dubrovinskaya, *J Mater Res* **14**(2), 456 (1999).
10. J. Mouzon, (2005) Licenciate Thesis Lulea university of Technology.
11. W. Sheng-Yue and L. Zu-Hong, *Materials Chemistry and Physics* **78**, 542 (2003).
12. T. E. Banach, C. Berti, E. Marianucci, M. Messori, F. Pilati, and M. Toseli, *Polymer* **42**, 7511 (2001).
13. H. Guo, W. Zhang, L. Lou, A Brioude, and J. Mugnier, *Thin Solid Films* **458**, 274 (2004).
14. K. Nakamoto, (1986) *Infrared and Raman Spectra of Inorganic and Coordination Compounds 4°* John Wiley & Sons 259–268, USA.
15. M. Aguilar-Frutis, M. Garcia, and C. Falcony, *Appl. Phys. Lett.* **72**(14), 1700 (1998).
16. M. Aguilar-Frutis, M. Garcia, C. Falcony, G. Plesch, and S Jimenez, *Thin solid films* **389**, 200 (2001).
17. H. Guo, W. Zhang, L. Lou, A Brioude, and J. Mugnier, *Thin Solid Films* **458**, 274 (2004).
18. Y. Repelin, C. Proust, E. Husson, and J. M. Beny, *Jornal of Solid State Chemistry* **118**, 163 (1995).
19. W. A. Pliskin and H. S. Lehman, *J. Electrochem. Soc.*, **112**, 1013 (1965).
20. J. Y. Choe, D. Ravichandran, S. M. Blomquist, K. W. Kirchner, E.W. Forsythe, and D.C. Morton, *Journal of Luminescence* **93**, 119 (2001).
21. G. Blasse and B. Grabmaier. *Luminescent Materials*. Springer-Verlag. (1994).
22. B. Lei, Y. Liu, G. Tang, Z. Ye, and C. Shi. *Materials Chemistry and Physics* **87**, 227 (2004).
23. M. A. Flores-Gonzalez, G. Ledoux, S. Roux, K. Lebbou, P. Perriat, and O. Tillement, *Journal of Solid State Chemistry* **178**, 989 (2005).
24. S. Ray, A. Patra, and P. Pramanik, *Optical Materials* **30**, 608 (2007).
25. J. C. G. Bunzli and G.R. Choppin, *Lanthanide Probes in Life, Chemical and Earth Sciences: Theory and Practices*, Elsevier, Amsterdam, Chap. 7, (1989).
26. A. Othonos, E. Lioudakis, and E. G. Nassiopoulou, *Nanoscale, Res. Lett.* **3**, 315 (2008).